SUPPLEMENTARY INFORMATION FOR

Single-cell analysis reveals fibroblast clusters linked to immunotherapy resistance in cancer

Yann Kieffer[1,2,10], Hocine R. Hocine[1,2,10], Géraldine Gentric[1,2,11], Floriane Pelon[1,2,11], Charles Bernard[1,2,11], Brigitte Bourachot[1,2], Sonia Lameiras[3], Luca Albergante[4], Claire Bonneau[1,2,5], Alice Guyard[6], Karin Tarte[7], Andrei Zinovyev[4], Sylvain Baulande[3], Gerard Zalcman[1,2,8], Anne Vincent-Salomon[9] and Fatima Mechta-Grigoriou[1,2,*]

[1] Institut Curie, Stress and Cancer Laboratory, Equipe labélisée par la Ligue Nationale contre le Cancer, PSL Research University, 26, rue d'Ulm, F-75248 Paris, France
[2] Inserm, U830, 26, rue d'Ulm, Paris, F-75005, France
[3] ICGex Next-Generation sequencing platform, Institut Curie, SIRIC, 26, rue d'Ulm, Paris, F-75005, France
[4] Institut Curie, PSL Research University, INSERM, U900, Mines Paris Tech, Paris, F-75005, France
[5] Department of Surgery, Institut Curie Hospital Group, 35 rue Dailly, 92210 Saint-Cloud, France
[6] Department of pathology Bichat Claude Bernard Hospital Group, Paris Diderot University, 46, rue Henri Huchard, 75877 PARIS cedex 18, France
[7] UMR U1236-MICMAC, Immunology and Cell Therapy Lab, Rennes University, 2, avenue du Pr Léon Bernard, 35043 Rennes, France
[8] Thoracic Oncology Department, CIC 1425-CLIP2, Bichat Claude Bernard Hospital Group, Paris Diderot University, 46, rue Henri Huchard, 75877 PARIS cedex 18, France
[9] Department of Diagnostic and Theragnostic Medicine, Institut Curie Hospital Group, 26, rue d'Ulm, F-75248 Paris, France

[10,11] These authors contributed equally to this work as 1st and 2nd authors, respectively

* Correspondence: Fatima Mechta-Grigoriou (ORCID Number: 0000-0002-3751-6989) Phone: +33 (0)1 56 24 66 53; Fax: +33 (0)1 56 24 66 50; E-mail address: fatima.mechta-grigoriou@curie.fr

Running title

FAP$^+$ CAF diversity and immunotherapy response

Figure S1 shows the first steps of the gating strategy used to isolate CAF-S1 clusters from breast cancer (BC) patients by multicolor flow cytometry and describes various properties of CAF-S1 clusters.

Figure S2 shows the identification of specific markers of CAF-S1 clusters used for subsequent analyses.

Figure S3 describes the gating strategies used to isolate T lymphocytes and NK cells, for subsequent correlation analyses with CAF-S1 clusters.

Figure S4 shows some properties of CAF-S1 clusters (ecm-myCAF and iCAF) established *in vitro.*

Table S1 describes the clinical and biological features of BC patients in the prospective and retrospective cohorts established in this study.

Table S2 describes the clinical and biological features of non-small cell lung cancer (NSCLC) patients treated by immunotherapy in the retrospective cohort established in this study.

Data S1 show specific pathways of each CAF-S1 cluster.

Data S2 shows the lists of genes that compose CAF-S1 cluster specific signatures.

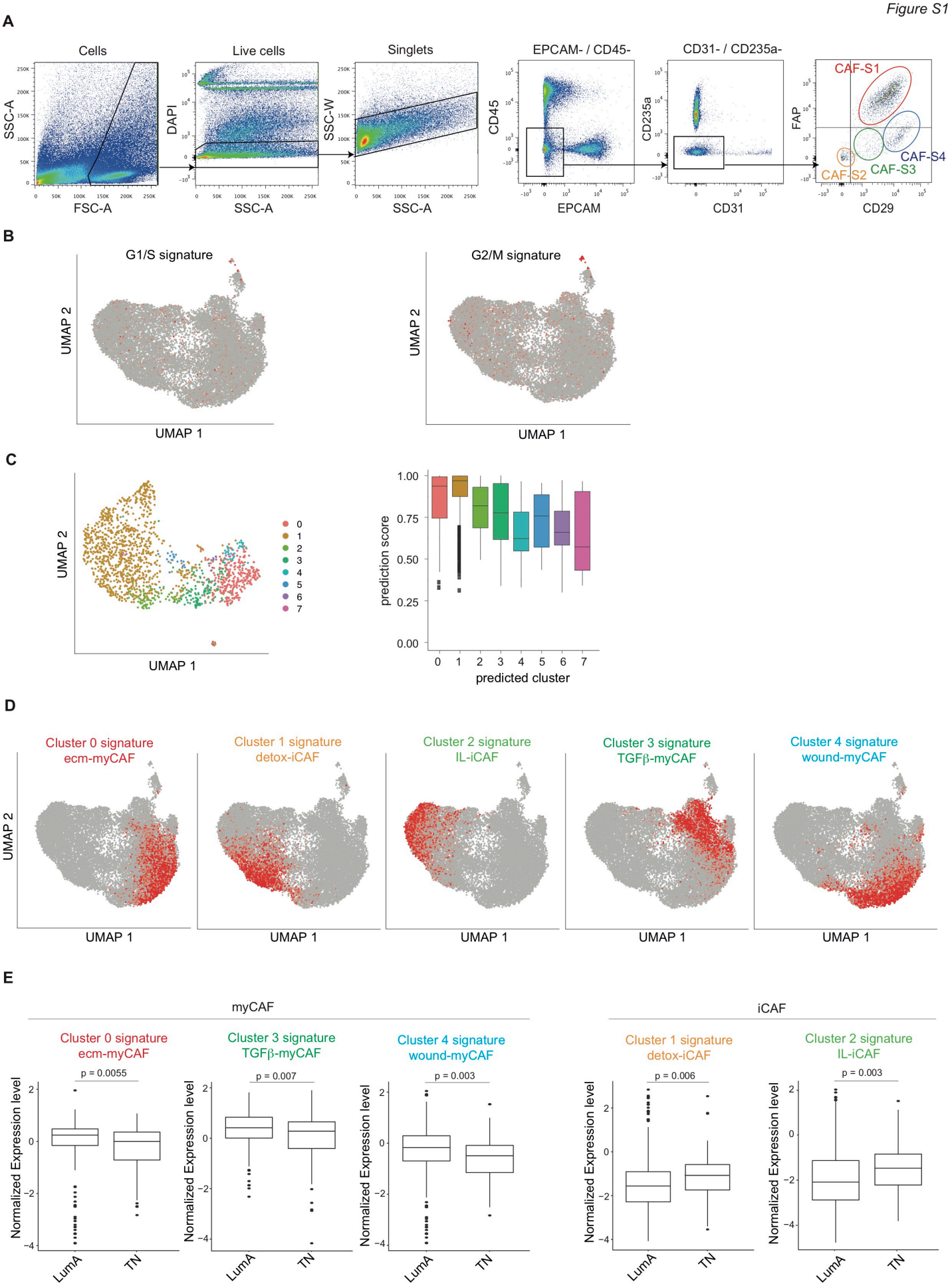
A
Cells
Live cells
Singlets
EPCAM- / CD45-
CD31- / CD235a-
SSC-A
FSC-A
DAPI
SSC-W
CD45
EPCAM
CD235a
CD31
FAP
CD29
CAF-S1
CAF-S2
CAF-S3
CAF-S4
B
G1/S signature
G2/M signature
UMAP 1
UMAP 2
C
prediction score
predicted cluster
D
Cluster 0 signature
ecm-myCAF
Cluster 1 signature
detox-iCAF
Cluster 2 signature
IL-iCAF
Cluster 3 signature
TGFβ-myCAF
Cluster 4 signature
wound-myCAF
E
myCAF
iCAF
p = 0.0055
p = 0.007
p = 0.003
p = 0.006
p = 0.003
Normalized Expression level
LumA
TN

Figure S1. Identification of CAF-S1 clusters

(**A**) Representative FACS plots showing the gating strategy used to isolate CAF-S1. Cells are first gated on $DAPI^-$ $EPCAM^-$ $CD45^-$ $CD31^-$ $CD235a^-$ to exclude dead, epithelial, hematopoietic, endothelial and red blood cells, respectively. FAP^{High} $CD29^{Med}$ cells are then selected as CAF-S1 fibroblasts. (**B**) Same UMAP plot as in (**Fig. 1A**) showing average z-score expression of cell cycle gene signatures (G1/S, Left and G2/M, Right). Signatures are from (1). (**C**) Left, UMAP plot of 1582 CAF-S1 fibroblasts from one BC patient (named as query dataset). Cells are colored by their predicted identity after applying Label Transfer algorithm implemented in Seurat. The scRNA-seq of 18 296 CAF-S1 cells from 7 BC patients was used as the reference dataset for predicted annotation of CAF-S1 clusters. Right, Boxplots showing the prediction score computed from Label Transfer algorithm for every cell in each CAF-S1 cluster of the query dataset. (**D**) UMAP plots of 18 296 CAF-S1 fibroblasts (as in **Fig. 1A**) showing average z-score of specific gene signatures (list of genes in **Data S2**) of the 5 most abundant CAF-S1 clusters**.** (**E**) Boxplots showing average expression of each CAF-S1 cluster signature among total CAF-S1 population (data normalized by FAP expression) in LumA and TN BC patients from the TCGA database (N = 328, with 231 LumA and 97 TN BC).

References:

1. Tirosh I, Izar B, Prakadan SM, Wadsworth MH, Treacy D, Trombetta JJ*, et al.* Dissecting the multicellular ecosystem of metastatic melanoma by single-cell RNA-seq. Science **2016**;352(6282):189-96 doi 10.1126/science.aad0501.

A

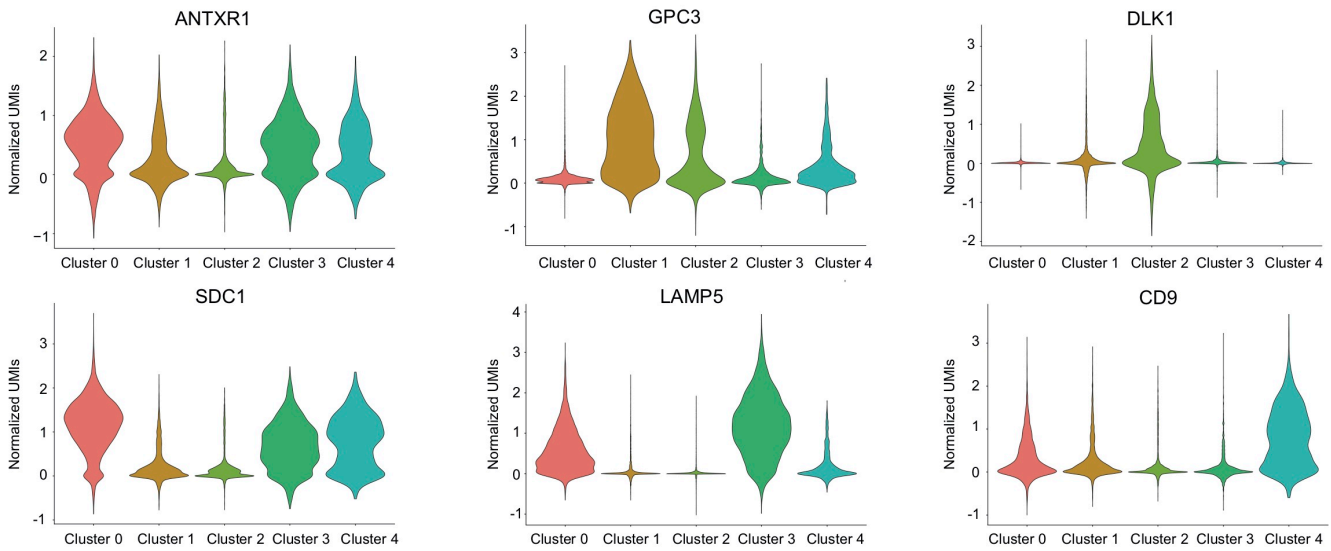
ANTXR1
GPC3
DLK1
SDC1
LAMP5
CD9
Normalized UMIs
Cluster 0
Cluster 1
Cluster 2
Cluster 3
Cluster 4

B

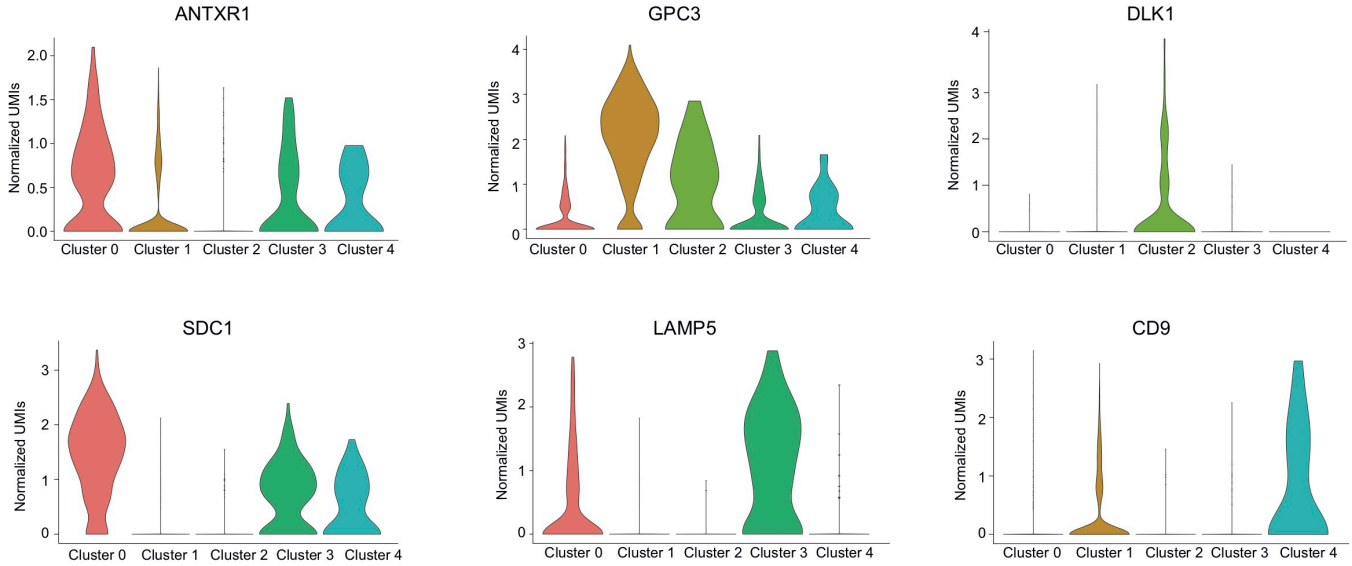
ANTXR1
GPC3
DLK1
SDC1
LAMP5
CD9
Normalized UMIs
Cluster 0
Cluster 1
Cluster 2
Cluster 3
Cluster 4

C

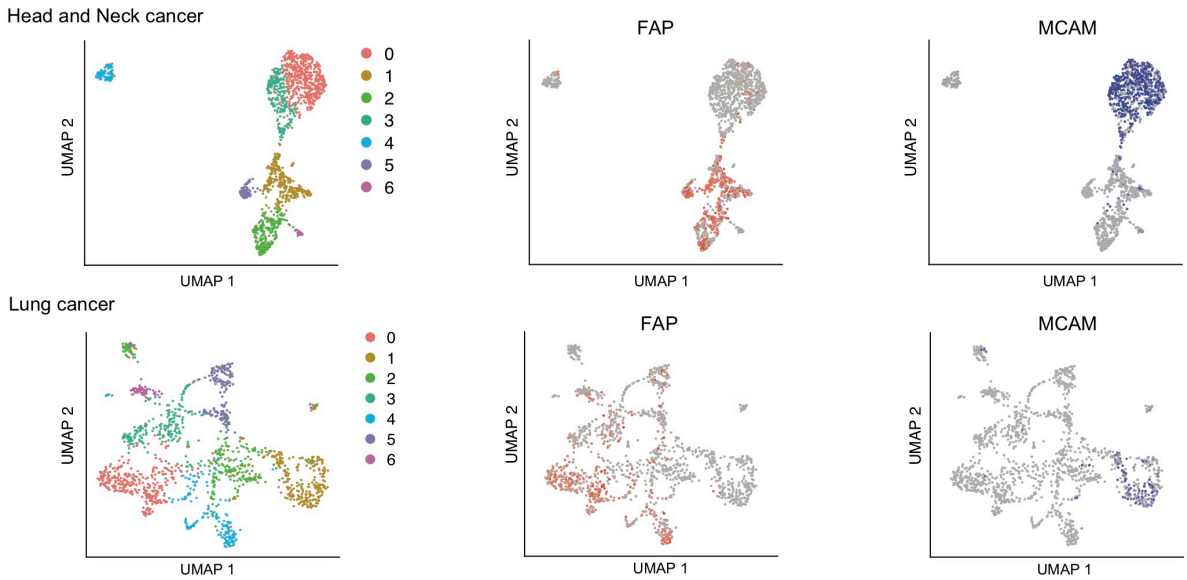
Head and Neck cancer
Lung cancer
FAP
MCAM
UMAP 1
UMAP 2
0
1
2
3
4
5
6

Figure S2. Identification of markers of CAF-S1 clusters for FACS analysis and selection of CAF-S1 from HNSCC and NSCLC scRNA-seq data

(**A**) Violin plots showing the distribution of expression (RNA levels from scRNA-seq from 18 296 CAF-S1 fibroblasts from 7 BC patients) of 6 genes encoding surface markers specific of each of the 5 most abundant CAF-S1 clusters. (**B**) Violin plots showing the expression level of the 6 CAF-S1 cluster markers in predicted CAF-S1 clusters defined by the Label Transfer algorithm in an additive scRNA-seq dataset (from 1582 CAF-S1 fibroblasts from 1 BC patient). (**C**) UMAP plots of 1422 fibroblasts from HNSCC (2) (Up) and 1465 fibroblasts from NSCLC (3) (Down). Colors highlight clusters obtained after applying Seurat v3 graph-based clustering. FAP (in red) and MCAM (in blue) markers are used to identify CAF-S1 (FAP^{Pos}) and CAF-S4 ($MCAM^{Pos}$) cells among the total fibroblasts, respectively. Following analyses were done on CAF-S1 (FAP^{Pos}) cells.

References:

2. Puram SV, Tirosh I, Parikh AS, Patel AP, Yizhak K, Gillespie S*, et al.* Single-Cell Transcriptomic Analysis of Primary and Metastatic Tumor Ecosystems in Head and Neck Cancer. Cell **2017**;171(7):1611-24 e24 doi 10.1016/j.cell.2017.10.044.
3. Lambrechts D, Wauters E, Boeckx B, Aibar S, Nittner D, Burton O*, et al.* Phenotype molding of stromal cells in the lung tumor microenvironment. Nat Med **2018**;24(8):1277-89 doi 10.1038/s41591-018-0096-5.

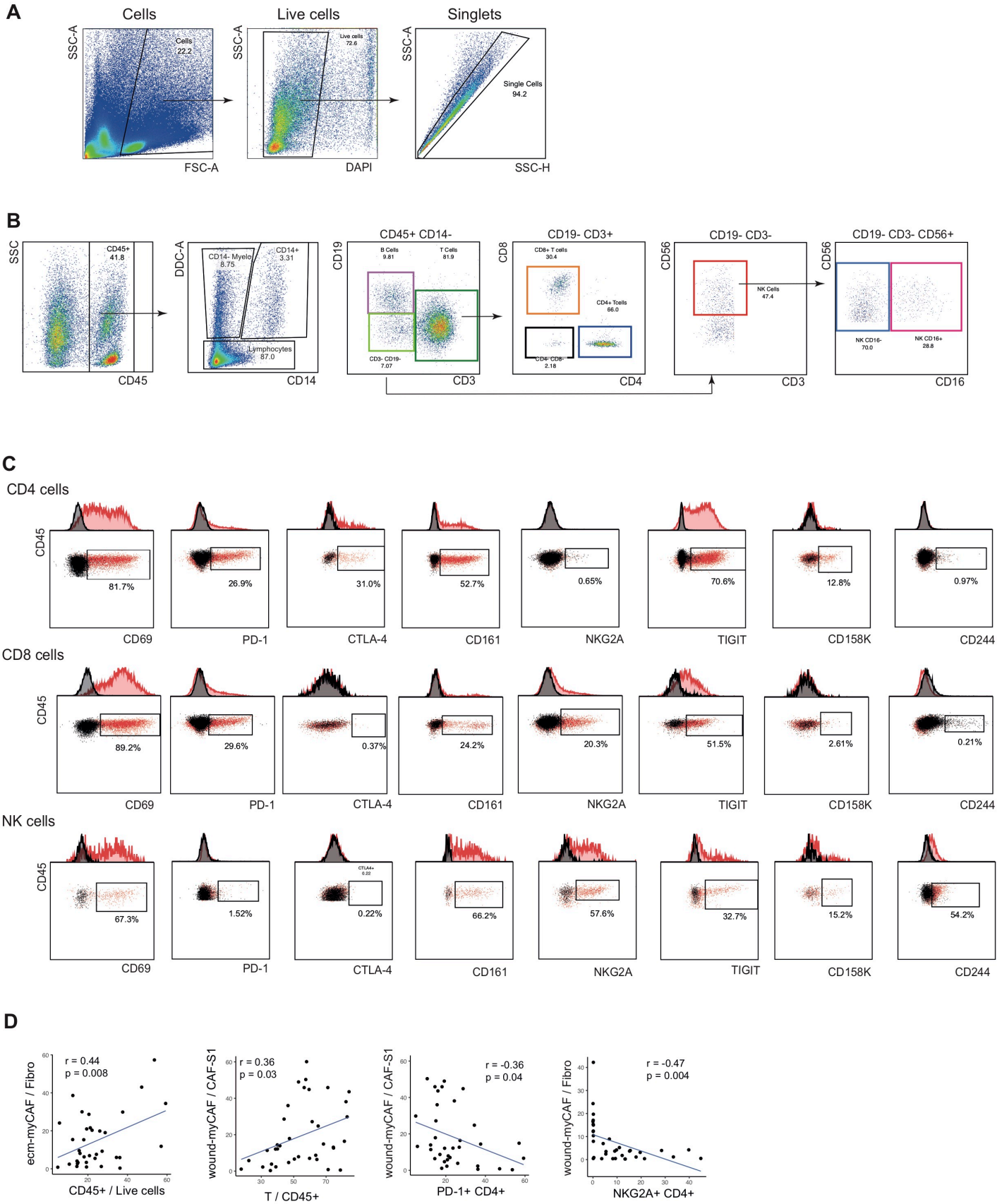
A
Cells
Live cells
Singlets
SSC-A
FSC-A
DAPI
SSC-H
Cells 22.2
Live cells 72.6
Single Cells 94.2
B
SSC
CD45
DDC-A
CD14
CD19
CD3
CD8
CD4
CD56
CD16
CD45+ 41.8
CD14- Myelo 8.75
CD14+ 3.31
Lymphocytes 87.0
CD45+ CD14-
B Cells 9.81
T Cells 81.9
CD3- CD19- 7.07
CD19- CD3+
CD8+ T cells 30.4
CD4+ Tcells 66.0
CD4- CD8- 2.18
CD19- CD3-
NK Cells 47.4
CD19- CD3- CD56+
NK CD16- 70.0
NK CD16+ 28.8
C
CD4 cells
CD8 cells
NK cells
CD45
CD69
PD-1
CTLA-4
CD161
NKG2A
TIGIT
CD158K
CD244
81.7%
26.9%
31.0%
52.7%
0.65%
70.6%
12.8%
0.97%
89.2%
29.6%
0.37%
24.2%
20.3%
51.5%
2.61%
0.21%
67.3%
1.52%
CTLA4+ 0.22
0.22%
66.2%
57.6%
32.7%
15.2%
54.2%
D
ecm-myCAF / Fibro
CD45+ / Live cells
r = 0.44
p = 0.008
wound-myCAF / CAF-S1
T / CD45+
r = 0.36
p = 0.03
PD-1+ CD4+
r = -0.36
p = 0.04
NKG2A+ CD4+
r = -0.47
p = 0.004

Figure S3. Correlation between CAF-S1 clusters and immune cells

(**A**) Representative FACS plots showing the gating strategy used to isolate immune cells. Singlet cells were first gated on $DAPI^-$ for identifying viable single cells. **(B)** Representative FACS plots showing the gating strategy used to isolate immune cells. Cells were first gated on $DAPI^-$ $CD45^+$ to identify alive hematopoietic cells. $CD14^-$ lymphocytes were next defined as T or B cells according to CD3 and CD19 expression, respectively. $CD3^+$ T cells were then sub-divided into $CD4^+$ or $CD8^+$ T lymphocytes. $CD3^-$ $CD19^-$ $CD56^+$ cells were assessed as NK cells and separated according to CD16 into cytotoxic NK ($CD56^+$ $CD16^+$) or non-cytotoxic NK cells ($CD56^+$ $CD16^-$). A representative patient is shown (N = 37 patients). (**C**) Representative FACS plots showing the expression of 8 checkpoint markers (CD69, PD-1, CTLA-4, CD161, NKG2A, TIGIT, CD158K and CD244) measured, for each patient, simultaneously at the surface of $CD4^+$ cells (upper panel), $CD8^+$ cells (middle panel) and NK cells (lower panel). Signals from specific antibodies are in red, and from corresponding isotype controls in black. Curves above show the corresponding distribution of mean fluorescent intensities, MFI. A representative patient is shown (N = 37 patients). (**D**) Detailed correlation plots between CAF clusters and immune cells, as indicated (N = 37 BC). P values from Pearson correlation test.

Figure S4

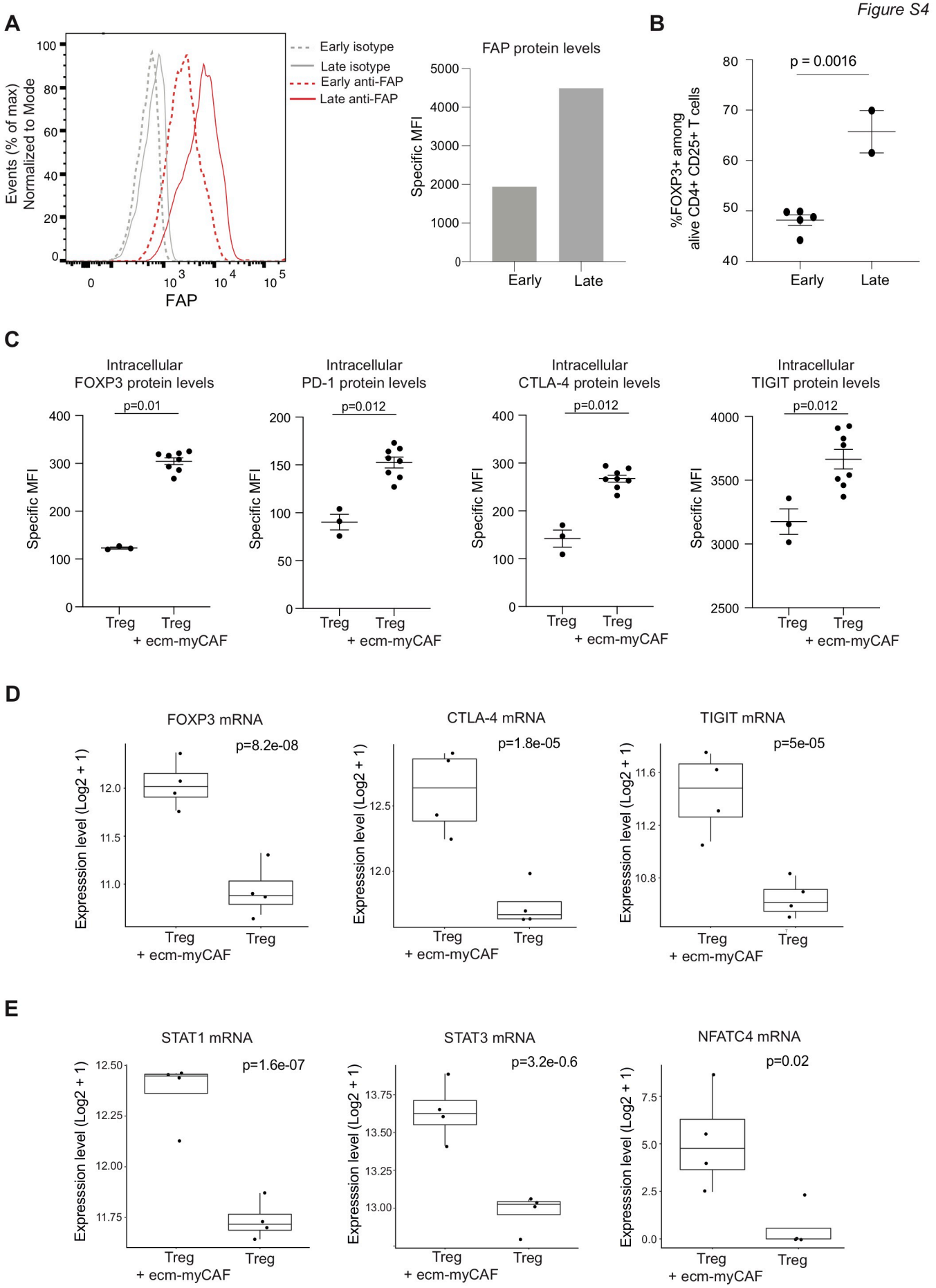
A
Events (% of max)
Normalized to Mode
FAP
Early isotype
Late isotype
Early anti-FAP
Late anti-FAP
FAP protein levels
Specific MFI
Early
Late
B
p = 0.0016
%FOXP3+ among
alive CD4+ CD25+ T cells
Early
Late
C
Intracellular
FOXP3 protein levels
p=0.01
Intracellular
PD-1 protein levels
p=0.012
Intracellular
CTLA-4 protein levels
p=0.012
Intracellular
TIGIT protein levels
p=0.012
Specific MFI
Treg
Treg
+ ecm-myCAF
D
FOXP3 mRNA
p=8.2e-08
CTLA-4 mRNA
p=1.8e-05
TIGIT mRNA
p=5e-05
Expression level (Log2 + 1)
E
STAT1 mRNA
p=1.6e-07
STAT3 mRNA
p=3.2e-0.6
NFATC4 mRNA
p=0.02

Figure S4. Fibroblasts isolated from juxta-tumors by spreading and maintained in plastic dishes acquire CAF-S1 properties

(A) Left, Representative FACS plots showing FAP protein levels (in red) in fibroblasts isolated by the spreading method from healthy juxta-tumors at early and late passages (Early, passage 2, dotted line and Late, passage 5, full line) of *in vitro* culture, compared to the corresponding isotype control (in grey). Right, Bar plot showing the specific mean fluorescent intensity of FAP (Specific MFI = MFI from the specific antibody – MFI from the isotype control) of fibroblasts isolated by the spreading method from healthy juxta-tumors at Early (P2) and Late (P5) passages of *in vitro* culture. **(B)** Percentage (%) of $CD4^+$ $CD25^+$ $FOXP3^+$ T lymphocytes normalized to survival in presence of fibroblasts from juxta-tumors at early (P2) and late (P5) passages of *in vitro* culture. Each dot represents an independent experiment (n = 7). Data are mean ± SEM. P value from Student t-test. (**C**) Dot plots showing the intracellular specific mean fluorescent intensity (speMFI) FOXP3, PD-1, CTLA-4 and TIGIT in $CD4^+$ $CD25^+$ T cells cultured alone (Left) or in presence of ecm-myCAF (Right). P values from Mann-Whitney test (N = 4 CAF-S1 primary cell lines). (**D**) Boxplots showing FOXP3, CTLA-4 and TIGIT mRNA levels in $CD4^+$ $CD25^+$ T cells cultured alone (Right) or in presence of ecm-myCAF (Left). P values from DESeq2 analysis (N = 8). (**E)** Same as in (**D**) for STAT and NFAT family members.

Table S1. Description of prospective and retrospective cohorts of BC patients (cohorts 1-3)

Table S1. Description of prospective cohorts of BC

		Prospective cohort 1 ssRNAseq - BC Patients	Prospective cohort 2 FACS - BC Patients	Prospective cohort 3 Primary cell lines - BC Patients
Number of cases		8	44	7
Age at surgery	**< 50 years**	3 (37.5%)	7 (15.9%)	3 (42.9%)
	> or = 50 years	5 (62.5%)	37 (84.1%)	4 (57.1%)
Multifocality	**no**	6 (75%)	37 (84.1%)	4 (57.1%)
	yes	2 (25%)	7 (15.9%)	2 (28.6%)
	NA	0 (0%)	0 (0%)	1 (14.3%)
Histological type	**ductal**	6 (75%)	33 (75%)	5 (71.4%)
	lobular	0 (0%)	4 (9.1%)	0 (0%)
	other	2 (25%)	7 (15.9%)	2 (28.6%)
Grade	**G1**	0 (0%)	9 (20.5%)	0 (0%)
	G2	6 (75%)	18 (40.9%)	5 (71.4%)
	G3	2 (25%)	16 (36.4%)	2 (28.6%)
	NA	0 (0%)	1 (2.3%)	0 (0%)
Tumor size	**pT1**	4 (50%)	21 (47.7%)	4 (57.1%)
	pT2	2 (25%)	18 (40.9%)	3 (42.9%)
	pT3	2 (25%)	4 (9.1%)	0 (0%)
	NA	0 (0%)	1 (2.3%)	0 (0%)
Lymph node metastases	**pN0**	4 (50%)	29 (65.9%)	4 (57.1%)
	pN1	3 (37.5%)	11 (25%)	1 (14.3%)
	pN2	0 (0%)	3 (6.8%)	2 (28.63%)
	pN3	1 (12.5%)	1 (2.3%)	0 (0%)
	NA	0 (0%)	0 (0%)	0 (0%)
Nottingham Prognostic Index	**excellent**	0 (0%)	0 (0%)	0 (0%)
	good	2 (25%)	15 (34.1%)	2 (28.6%)
	moderate	5 (62.5%)	26 (59.1%)	5 (71.4%)
	poor	1 (12.5%)	2 (4.5%)	0 (0%)
	NA	0 (0%)	1 (2.3%)	0 (0%)
Estrogen receptor (RO)	**no**	2 (25%)	9 (20.5%)	1 (14.3%)
	yes	6 (75%)	34 (77.3%)	6 (85.7%)
	NA	0 (0%)	1 (2.3%)	0 (0%)
Progesterone receptor (RP)	**no**	2 (25%)	13 (29.5%)	3 (42.9%)
	yes	6 (75%)	30 (68.2%)	4 (57.1%)
	NA	0 (0%)	1 (2.3%)	0 (0%)
HER2 amplification/overexpression	**no**	8 (100%)	39 (88.6%)	7 (100%)
	yes	0 (0%)	4 (9.1%)	0 (0%)
	NA	0 (0%)	1 (2.3%)	0 (0%)
Surgical treatment	**lumpectomy**	4 (50%)	26 (59.1%)	5 (71.4%)
	mastectomy	4 (50%)	18 (40.9%)	2 (28.6%)
Hormone therapy	**no**	2 (25%)	9 (20.4%)	1 (14.3%)
	yes	6 (75%)	35 (79.5%)	6 (85.7%)
	NA	0 (0%)	0 (0%)	0 (0%)
Adjuvant chemotherapy	**no**	2 (25%)	22 (50%)	3 (42.9%)
	yes	6 (75%)	21 (47.7%)	4 (57.1%)
	NA	0 (0%)	1 (2.3%)	0 (0%)
Radiotherapy	**no**	0 (0%)	9 (20.5%)	0 (0%)
	yes	8 (100%)	33 (75%)	7 (100%)
	NA	0 (0%)	2 (4.5%)	0 (0%)
Trastuzumab	**no**	8 (100%)	41 (93.2%)	7 (100%)
	yes	0 (0%)	3 (6.8%)	0 (0%)
	NA	0 (0%)	0 (0%)	0 (0%)
Relapse	**no**	8 (100%)	43 (97.7%)	7 (100%)
	yes	0 (0%)	1 (2.3%)	0 (0%)
Survival	**alive**	8 (100%)	44 (100%)	7 (100%)
	deceased	0 (0%)	0 (0%)	0 (0%)

Table S2. Description of the retrospective cohort of NSCLC patient treated by immunotherapy (cohort 4)

NSCLC samples were from the routine diagnostic samples stored in the Pathology Department of Bichat Hospital, from patients treated by immuno-oncology drugs. All patients received 2nd or 3rd line immunotherapy first cycle, according to drug registrations at that period of time and on-going clinical trials, from 28 July 2015 to 20 Feb. 2018. Efficacy of immuno-oncology treatment was assessed every 8 to 12 weeks by whole body CT-scan, according to RECIST v.1.1 criteria. All clinical data were retrieved from patients electronic files. Histological subtypes of non-small cell lung cancer samples were determined according to the current World Health Organization 2015 classification, on formalin-fixed paraffin-embedded tissue sections, stained with haematoxylin, from bronchial endoscopy or CT-guided transthoracic biopsy samples. Squamous-Cell Cancer diagnosis was supported by p40 positive and TTF-1 (thyroid transcription factor 1) negative immunostaining. Non-squamous lung cancer included both adenocarcinoma showing Alcian blue positive staining (for mucin tumor cell content) and/or nuclear TTF-1 positive immunostaining, and large-cell carcinoma devoid of mucin secretion, with p40- and TTF-1-negative immunostaining. Two samples exhibited mixt features of squamous and adenocarcinoma differentiation. The two stage IIIB patients, according to the 8th TNM staging system, had non resectable lung tumor, and have contra-indication to radiation therapy . *PD-L1 staining was performed and interpreted by AG, on 4-μm paraffin-embedded sections, from diagnosis, pre-treatment biopsy samples, containing at least 200 tumor cells, using Cell Signaling Technology E1L3N commercially available clone, on the Leica Bond platform.

**EOCG (Eastern Cooperative Oncology Group) performance status was assessed at time of first immunotherapy cycle according to (4).

References:

4. Oken MM, Creech RH, Tormey DC, Horton J, Davis TE, McFadden ET, *et al.* Toxicity and response criteria of the Eastern Cooperative Oncology Group. Am J Clin Oncol **1982**;5(6):649-55.

Table S2. description of the retrospective cohort of NSCLC patient treated by immunotherapy (cohort 4)

		Patients
Number of cases		70
Mean Age (year) (min-max)		62.5 (40-83)
Gender (%)	**Female**	20 (28.6%)
	Male	50 (71.4%)
Tumor type (%)	**non-Squamous cell carcinoma**	47 (67.1%)
	Squamous cell carcinoma	21 (30.0%)
	Adenocarcinoma / squamous	2 (2.9%)
Stage (%)	**IIIB**	2 (2.9%)
	IV	68 (97.1%)
Smoking status (%)	**Active smokers**	37 (52.9%)
	Former smokers	29 (41.4%)
	Never smokers	4 (5.7%)
Pack-Years (mean) (min-max)		41.15 (0-150)
Metastasis sites (%)	**Brain**	23 (32.9%)
	Liver	9 (12.9%)
	Bone	27 (38.6%)
	Suprarenal gland	20 (28.6%)
nb. of metastastic sites (%)	**0**	2 (2.9%)
	1	33 (47.1)
	≥2	35 (50.0)
PD-L1 staining (%)*	**≥50%**	30 (42.9)
	1-49%	21 (30.0)
	<1%	14 (20.0)
	Not done	5 (7.1)
i.o. drug (%)	**Nivolumab**	56 (80.0)
	Pembrolizumab	5 (7.1)
	Nivo+ipilumumab	8 (11.4)
	Nivo+chemo	1 (1.4)
line of treatment	**1L**	20 (28.6)
	2L	37 (52.9)
	>3L	13 (18.6)
ECOG performance status**	**PS= 0-1**	43 (61.4)
	PS=2-3	27 (38.6)

Data S1. Transcriptomic profile of the 8 CAF-S1 clusters

Pathway analysis using Metascape of the genes differentially expressed in the 8 CAF-S1 clusters. Up-regulated genes in one specific cluster compared to the others (one *versus* all) were defined using Wilcoxon rank-sum test (adjusted P value ≤ 0.05).

Data S2. List of genes that compose CAF-S1 cluster-specific signatures

1st Tab: CAF-S1 cluster-specific signatures were defined for clusters 0 to 5. For each cluster, differential expression analysis was performed against the other clusters (one *versus* all) using Wilcoxon rank-sum test. Genes were conserved in signature of each CAF-S1 cluster if adjusted P value was below 0.05. As we also used these signatures for detecting CAF-S1 clusters in RNA-seq data from single cells and bulk of different cancer types, we eliminated genes that were also expressed in melanoma, NSCLC and HNSCC cancer cells to avoid any signal from cancer cells and analyzed strictly information coming from CAF-S1 clusters. To assess the level of expression of each gene in tumor cells, scRNA-seq data of tumor cells from NSCLC, melanoma and HNSCC (1-3) were analyzed. A CAF-S1 cluster gene showing an average expression level higher than 1 in tumor cells was considered as expressed. Genes were kept in CAF-S1 clusters signatures only if the fraction of positive cells in melanoma, NSCLC and HNSCC cancer cells was less than 10%.

2nd Tab: Gene signatures of CAF-S1, CAF-S1 clusters and normal fibroblasts. CAF-S1 global signature was initially published in (5). Among these genes, those expressed in tumor cells were excluded if more than 10% of tumor cells show an expression level higher than 1 (see also Methods, #*Gene signatures of CAF-S1, CAF-S1 clusters*). The first 100 most significant genes were considered for the CAF-S1-specific signature. The normal fibroblast signature was defined by the genes significantly up-regulated in normal fibroblasts (FAP^{Neg} $CD29^{Med}$ SMA^{Neg}) isolated from healthy juxta-tumor tissues, compared to CAF-S1 fibroblasts isolated from BC. Genes that are expressed in tumor cells were excluded from the signature, following the same strategy as this one described above. Cytolytic index was defined as the geometric mean of granzyme A (GZMA) and perforin (PRF1) gene expression, as described in (6).

References:

5. Costa A, Kieffer Y, Scholer-Dahirel A, Pelon F, Bourachot B, Cardon M, *et al.* Fibroblast Heterogeneity and Immunosuppressive Environment in Human Breast Cancer. Cancer Cell **2018**;33(3):463-79 e10 doi 10.1016/j.ccell.2018.01.011.

6. Rooney MS, Shukla SA, Wu CJ, Getz G, Hacohen N. Molecular and genetic properties of tumors associated with local immune cytolytic activity. Cell **2015**;160(1-2):48-61 doi 10.1016/j.cell.2014.12.033.